Asymmetric distribution of Echinoid defines the epidermal leading edge during *Drosophila* dorsal closure

Caroline Laplante and Laura A. Nilson

Department of Biology, McGill University, Montréal, Quebec H3A 1B1, Canada

During *Drosophila melanogaster* dorsal closure, lateral sheets of embryonic epidermis assemble an actomyosin cable at their leading edge and migrate dorsally over the amnioserosa, converging at the dorsal midline. We show that disappearance of the homophilic cell adhesion molecule Echinoid (Ed) from the amnioserosa just before dorsal closure eliminates homophilic interactions with the adjacent dorsal-most epidermal (DME) cells, which comprise the leading edge. The resulting planar polarized distribution of Ed in the DME cells is essential for the localized accumulation of actin regulators and for actomyosin cable formation at the leading edge and for the polarized localization of the scaffolding protein Bazooka/PAR-3. DME cells with uniform Ed fail to assemble a cable and protrude dorsally, suggesting that the cable restricts dorsal migration. The planar polarized distribution of Ed in the DME cells thus provides a spatial cue that polarizes the DME cell actin cytoskeleton, defining the epidermal leading edge and establishing its contractile properties.

Introduction

Tissue morphogenesis is driven by coordinated cell movements, shape changes, and rearrangements, which in turn depend on local control of actin dynamics (Zallen, 2007; Harris et al., 2009). Elucidating the spatial cues that define the cell populations that will undergo these changes and that lead to the required remodeling of the actin cytoskeleton is thus important for understanding the regulation of epithelial movements in vivo. An important model for epithelial morphogenesis is the process of dorsal closure during *Drosophila melanogaster* embryogenesis, in which two lateral sheets of epidermis move dorsally over the extraembryonic amnioserosa and converge at the dorsal midline (Young et al., 1993; Kiehart et al., 2000; Jacinto et al., 2001; Harden, 2002; Jacinto et al., 2002b). These movements are the result of contractile forces and cell shape changes in both the epidermis and amnioserosa, which culminate in direct filopodial interactions between the opposing epidermal edges that ultimately establish a continuous epidermis (Kiehart et al., 2000; Jacinto et al., 2002b; Franke et al., 2005; Solon et al., 2009; Blanchard et al., 2010).

At the onset of dorsal closure, the dorsal-most epidermal (DME) cells, which lie at the leading edge of the epidermal sheets and therefore abut the amnioserosa, elongate within the dorsal–ventral (DV) plane of tissue (Ring and Martinez Arias, 1993; Young et al., 1993; Kiehart et al., 2000). This planar polarity of their shape is also reflected at the molecular level by the planar polarized localization of several factors, such as actin regulators that become enriched at tricellular junctions along the DME cell leading edge and septate junction proteins that are absent from the leading edge (Kaltschmidt et al., 2002; Homem and Peifer, 2008; Narasimha et al., 2008). The DME cells also accumulate filamentous actin (F-actin) and nonmuscle myosin II (hereafter referred to as myosin II) at their leading edge, forming a supracellular actomyosin cable that confers contractile properties upon the leading edge and provides one of the forces orchestrating the tissue movements that

Correspondence to Laura A. Nilson: laura.nilson@mcgill.ca

Caroline Laplante's present address is Dept. of Molecular, Cell, and Developmental Biology, Yale University, New Haven, CT 06520.

Abbreviations used in this paper: ANC, actin-nucleating center; AP, anterior–posterior; Baz, Bazooka/PAR-3; Dia, Diaphanous; DME, dorsal-most epidermal; DV, dorsal–ventral; Ed, Echinoid; Ena, Enabled/VASP; F-actin, filamentous actin; Fmi, Flamingo; MARCM, mosaic analysis with a repressible cell marker; MHC, myosin heavy chain; pAS, peripheral amnioserosa; pMLC, phosphorylated myosin II light chain; UAS, upstream activating sequence.

The Rockefeller University Press $30.00
J. Cell Biol. Vol. 192 No. 2 335–348
www.jcb.org/cgi/doi/10.1083/jcb.201009022

drive dorsal closure (Young et al., 1993; Kiehart et al., 2000; Jacinto et al., 2002b).

Although the morphological and molecular properties of the DME cells have been extensively characterized and their contribution to dorsal closure well studied, how their identity and polarity are established remains unclear. Positionally, they can be recognized by their location at the leading edge of the tissue, but the molecular information that provides the spatial cue distinguishing the DME cells from other epidermal cells and how this information leads to their planar polarization is not understood. Wingless signaling is required for DME cell planar polarization but does not provide the positional input that establishes this polarity (Kaltschmidt et al., 2002). JNK signaling has been implicated in planar polarity in other tissues and is required for normal dorsal closure (Glise et al., 1995; Riesgo-Escovar et al., 1996; Sluss et al., 1996; Strutt et al., 1997; Boutros et al., 1998; Noselli and Agnès, 1999) but does not appear to play an instructive role in DME cell polarization (Glise et al., 1995; Kaltschmidt et al., 2002; Stronach and Perrimon, 2002).

As a candidate for such a cue, we have investigated the transmembrane protein Echinoid (Ed; Bai et al., 2001; Wei et al., 2005; Laplante and Nilson, 2006). Clones of *ed* mutant epithelial cells form smooth actomyosin-rich interfaces with neighboring Ed-expressing cells, suggesting that a contractile actomyosin cable assembles at the border between cells that express Ed and those that lack Ed. Ed undergoes homophilic interactions via its extracellular domain, which contains seven immunoglobulin domains and a fibronectin type III domain, which is consistent with a role for Ed in mediating interactions between neighboring cells (Bai et al., 2001; Islam et al., 2003; Spencer and Cagan, 2003; Wei et al., 2005; Laplante and Nilson, 2006). An endogenous interface between Ed-expressing and nonexpressing cells arises in the embryo during dorsal closure when Ed expression is lost from the amnioserosa but persists in the epidermis, but whether this differential expression of Ed leads to cable formation at the leading edge remains unclear (Laplante and Nilson, 2006; Lin et al., 2007).

In this study, we show that ectopic expression of Ed in the amnioserosa abolishes actomyosin cable formation at the DME cell leading edge, indicating that in a normal developmental context, juxtaposition of cells with and without Ed leads to cable formation at their interface. We also show that loss of Ed from the amnioserosa eliminates Ed homophilic interactions at the epidermis/amnioserosa interface, resulting in the disappearance of Ed from the DME cell leading edge and a planar polarized distribution of Ed within the DME cells. This polarized distribution, rather than the presence or absence of Ed itself, is required for the localization of actin regulators to the leading edge, where they mediate actomyosin cable assembly. The Ed intracellular domain, but not its C-terminal PDZ-binding motif, is required for this function. The planar polarized distribution of Ed is also required for the planar polarized localization of the scaffolding protein Bazooka/PAR-3 (Baz) in the DME cells, and this polarity precedes cable formation, suggesting that Ed may function by regulating Baz localization. We also show that DME cells lacking a cable exhibit enhanced dorsal migration, suggesting that the cable restricts the forward movement of the leading edge. Collectively, our data suggest that the disappearance of Ed from the amnioserosa provides the initial spatial cue that molecularly distinguishes the cells at the dorsal edge of the epidermis; the resulting loss of homophilic interaction generates a polarized distribution of Ed in the DME cells, which in turn mediates proper localization of Baz and actin regulators, which direct localized actomyosin cable assembly to the leading edge. The homophilic binding properties of Ed thus allow it to function as a "sensor," allowing a cell to detect whether its neighbors also express Ed, thus providing information to the cell about its position within the tissue.

Results

Differential expression of Ed is essential for actomyosin cable assembly

During embryogenesis, Ed is initially detectable uniformly at the apical domain of all epidermal and amnioserosa cells but just before dorsal closure, while the germ band is fully extended (embryonic stage 11), levels of Ed begin to decrease in the amnioserosa (Fig. 1, A–C). During the initiation phase of dorsal closure (stage 12), the peripheral amnioserosa (pAS) cells, those that abut the DME cells, are the first to exhibit complete loss of Ed (Fig. 1, D and D′). By the epithelial sweeping phase (stage 13), when the actomyosin cable is assembled at the DME cell leading edge (Jacinto et al., 2002b), Ed is absent throughout the amnioserosa (Fig. 1, E and E′; Laplante and Nilson, 2006; Lin et al., 2007). Ed remains undetectable during the zippering (stage 14) and termination (stage 15) phases (Fig. 4 C and not depicted). Loss of Ed from the amnioserosa thus coincides temporally with the appearance of the cable, which is consistent with a model in which loss of Ed from the amnioserosa leads to differential expression of Ed between the amnioserosa and epidermis, which in turn induces the assembly of a contractile actomyosin cable at their interface (Laplante and Nilson, 2006).

To test this hypothesis, we used the upstream activating sequence (UAS)/GAL4 system (Brand and Perrimon, 1993) and an amnioserosa-specific GAL4 driver (c381-GAL4) to determine whether ectopically expressing Ed in the amnioserosa would block cable formation. Expression of a full length Ed transgene (Ed-Full) in the amnioserosa resulted in levels of ectopic expression comparable with endogenous levels in the epidermis (Fig. 1 G). Interestingly, however, the pAS cells often failed to express Ed-Full (Fig. 1, G [arrow] and H). This pattern does not result from variable expression of the c381-GAL4 driver (see Fig. S1), and the underlying cause remains unclear. However, the presence of these Ed nonexpressing cells provides an internal control that allows us to directly compare interfaces between DME cells and amnioserosa cells that express or lack Ed. Consistent with our model, actomyosin cable formation in the DME cells was abolished when Ed-Full was expressed in the adjacent pAS cells (Fig. 1 G, arrowhead) but remained detectable when the adjacent pAS cell failed to express the transgene (Fig. 1 G, arrow).

To investigate this effect further, we tested the requirement for the Ed intracellular region, which contains no obvious domains except for a PDZ-binding motif at the C terminus (Bai et al., 2001). A transgenic form of Ed lacking the C-terminal PDZ-binding motif (Ed-ΔP; Fig. 1 F) was variably expressed in

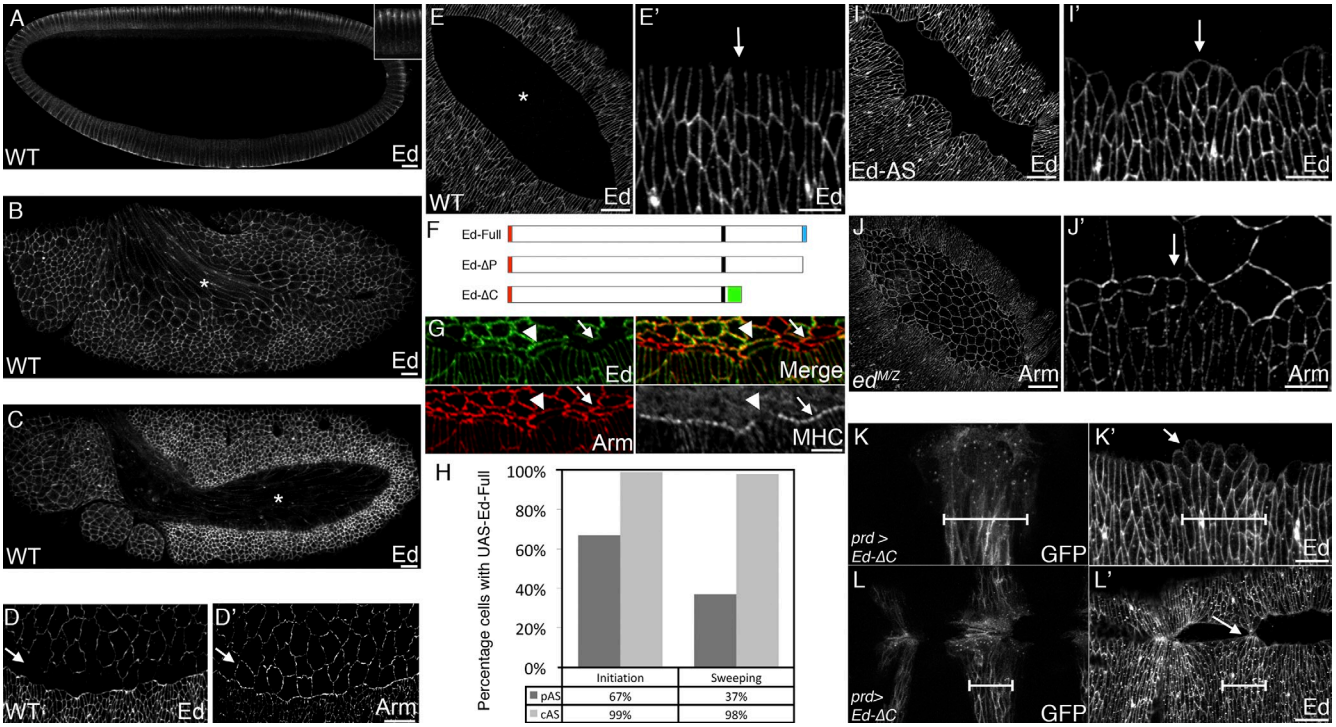

Figure 1. **Ectopic expression of Ed in the amnioserosa blocks actomyosin cable assembly and retains Ed at the DME cell leading edge.** (A–C) Wild-type (WT) embryos stained for Ed. (A) Cellularization stage; inset shows magnified view of dorsal cells. (B) Stage 8 (germ band extension). Ed is detectable in all epidermal and amnioserosa (*) cells. (C) Stage 11 (extended germ band). Ed levels are decreased in the amnioserosa (*). (D and D′) Wild-type (initiation phase) embryo stained for Ed (D) and Armadillo (Arm; D′). The pAS cells have little or no detectable Ed (arrows), whereas the remaining amnioserosa cells still show some Ed. (E and E′) Wild-type (sweeping phase) embryo stained for Ed. (E′) Magnified view of the DME cells. Ed is absent from the amnioserosa (*) and DME cell leading edge (arrow). (F) Diagram of transgenic Ed proteins. (G) Zippering phase embryo expressing Ed-Full in the amnioserosa under the control of c381-GAL4, stained for Ed (green), Arm (red), and MHC (gray). As shown by the colocalization of Ed and Arm, most pAS cells fail to express Ed-Full (merge, arrow), but one pAS cell expresses Ed (merge, arrowhead). The DME cells adjacent to the latter fail to assemble an actomyosin cable (MHC, arrowhead). (H) Percentage of peripheral (pAS) or central (cAS) amnioserosa cells expressing Ed-Full. For initiation, n = 151 pAS cells and 598 cAS cells; for sweeping, n = 120 pAS cells and 522 cAS cells. (I and I′) Sweeping phase embryo expressing Ed-ΔC in the amnioserosa and stained for Ed. (I′) Magnified view of the leading edge. Endogenous Ed is maintained at the DME cell leading edge, and the DME cells fail to elongate along the DV axis (arrow). (J and J′) Sweeping phase $ed^{M/Z}$ embryo stained for Arm. (J′) Magnified view of the DME cells. The DME cells (arrow) fail to elongate along the DV axis. (K and K′) Sweeping phase embryo expressing Ed-ΔC in *paired* expression stripes (bars) stained for GFP (K) and Ed (K′). The DME cells adjacent to the pAS cells expressing Ed-ΔC maintain endogenous Ed at their leading edge and gain a migrational advantage over the flanking DME cells (K′, arrow). (L and L′) Termination phase embryo expressing Ed-ΔC in *paired* expression stripes (bars) stained for GFP (L) and Ed (L′). Ed-ΔC expressing cells make premature contact at the dorsal midline (L′, arrow). The brightness of A was increased using the "Levels" function in Photoshop (Adobe). See Figs. S1 and S2. Bars: (A–E, I, J, and L′) 20 µm; (E′, G, I′, J′, and K′) 10 µm.

the pAS cells but capable of abolishing cable formation (not depicted) and was thus indistinguishable from Ed-Full in this assay. We then generated a transgene encoding a form of Ed lacking most of the intracellular domain and bearing a C-terminal GFP tag (Ed-ΔC; Fig. 1 F). Unlike Ed-Full, Ed-ΔC is detectable uniformly in amnioserosa cells, including the pAS cells, throughout dorsal closure (Fig. S1). To reflect this uniform expression of Ed in the amnioserosa, we refer to these as Ed-AS embryos. However, like Ed-Full, expression of Ed-ΔC in the amnioserosa abolished actomyosin cable formation: the leading edge did not exhibit enrichment of the actomyosin cable markers F-actin, myosin heavy chain (MHC), and active phosphorylated myosin II light chain (pMLC; Fig. 2, B, E, and H) and appeared markedly jagged (Fig. 1, I and I′) compared with wild type (Fig. 1, E and E′; and Fig. 2, A, D, and G), which is consistent with a failure of actomyosin cable formation and a lack of tension at the leading edge. In addition, the elongation of the DME cells along the DV axis, which has been linked to the tension exerted by the contractile actomyosin cable (Jacinto et al., 2002a), fails to occur in Ed-AS embryos (Fig. 1 I′ and Fig. S2). In contrast, these embryos exhibit little or no defect in the elongation of the more-ventral rows of epidermal cells (Fig. S2), which is thought to be regulated by the JNK and Decapentaplegic pathways and independent of the actomyosin cable (Riesgo-Escovar and Hafen, 1997; Ricos et al., 1999). The DME cells also exhibited few detectable filopodia (Fig. 2 B), which in wild-type embryos are abundant and protrude from the leading edge (Fig. 2 A; Jacinto et al., 2000; Kaltschmidt et al., 2002).

We also used the *paired*-GAL4 driver (Yoffe et al., 1995) to express Ed-ΔC in segmental stripes that extend around the entire circumference of the embryo, including both epidermal and amnioserosa cells, allowing us to compare within the same embryo the phenotype of DME cells adjacent to amnioserosa cells without Ed to DME cells adjacent to amnioserosa cells with Ed (the Ed-AS stripe; Fig. 1 K, arrow). The DME cells of the Ed-AS stripe adopt a fan shape with their leading edge splayed wide along the anterior–posterior (AP) axis compared with the narrow leading edge of the wild-type cells (n = 37;

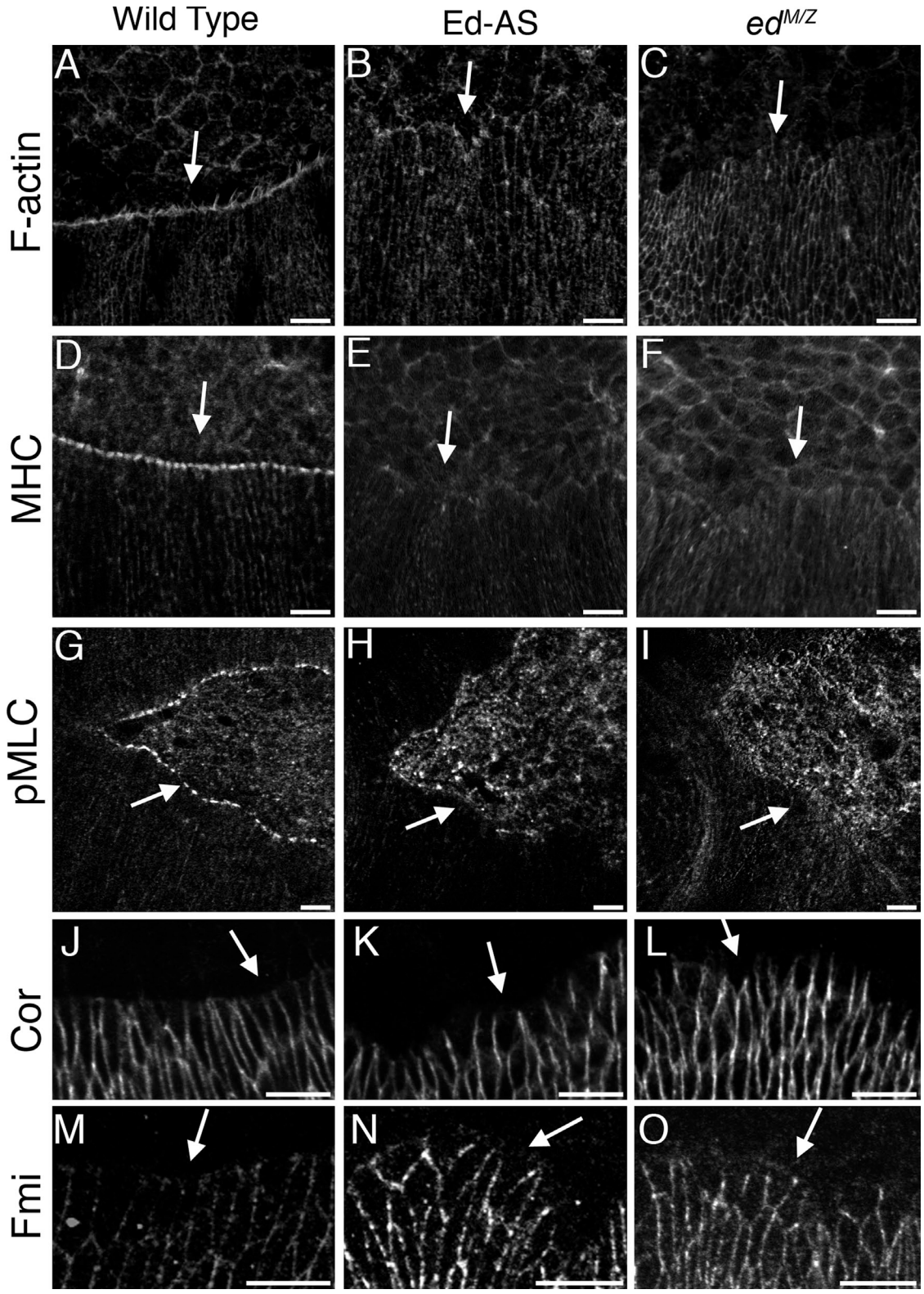

Figure 2. **Polarized Ed distribution is essential for actomyosin cable assembly but not for the overall planar polarity of the DME cells.** Zippering phase wild-type embryos (A, D, G, J, and M), Ed-AS embryos (B, E, H, K, and N), and $ed^{M/Z}$ embryos (C, F, I, L, and O) stained to visualize F-actin (A–C), MHC (D–F), pMLC (G–I), Coracle (Cor; J–L), and Fmi (M–O). Arrows point to the leading edge of the DME cells. Bars, 10 µm.

Fig. 1 K′, arrow). These cells also appear to acquire a migration advantage and extend further dorsally than their neighbors (Fig. 1 K′), and in later stages, they establish premature contacts at the dorsal midline (Fig. 1, L and L′). This observation suggests that the actomyosin cable restrains rather than promotes forward movement of the leading edge (Jacinto et al., 2002a).

Strikingly, the phenotype of Ed-AS embryos appears identical to that of embryos lacking both maternal and zygotic *ed* contributions ($ed^{M/Z}$ embryos; Laplante and Nilson, 2006; Lin et al., 2007). The leading edge of $ed^{M/Z}$ embryos is not smooth (Fig. 1, J and J′) and does not exhibit actomyosin cable markers or filopodia (Fig. 2, C, F, and I), and DME cell elongation is similarly impaired (Fig. S2). These observations support the hypothesis that the juxtaposition of cells with and without Ed leads to assembly of an actomyosin cable at their interface. If we eliminate this differential Ed expression between the epidermis and amnioserosa either by ectopic Ed expression in the amnioserosa or removal of Ed from the epidermis, actomyosin cable formation at the leading edge is abolished.

Ectopic Ed expression in the amnioserosa maintains endogenous Ed at the leading edge

To investigate how such different genetic manipulations might both result in such a similar effect on the leading edge, we looked at the distribution of Ed in the DME cells. In wild type, the loss of Ed from the amnioserosa is followed by the disappearance of Ed from the epidermal leading edge (Fig. 1, D and E′; and see Fig. 4, A and B; Laplante and Nilson, 2006; Lin et al., 2007). We therefore asked whether the disappearance of Ed from the leading edge is because of the loss of stabilizing homophilic interactions with Ed in the neighboring amnioserosa cells. We analyzed Ed-AS embryos because Ed-ΔC is uniformly expressed throughout the amnioserosa and is sufficient to inhibit cable formation and because it is not recognized by our anti-Ed antiserum, allowing us to specifically visualize the effect on endogenous Ed in the epidermis. In Ed-AS embryos, endogenous Ed is detectable at the leading edge of the DME cells (Fig. 1 I′, arrow), indicating that expression of Ed-ΔC by the amnioserosa cells is sufficient to maintain endogenous Ed at the leading edge, presumably through homophilic interaction. Similar results were obtained for both Ed-Full and Ed-ΔP (Fig. 1 G and not depicted), except where the adjacent pAS cells failed to express the transgenes.

These observations offer a potential explanation for the strikingly similar loss of actomyosin cable formation in both $ed^{M/Z}$ and Ed-AS embryos, even though they differ markedly in terms of Ed expression. In wild type, when Ed is lost from the epidermal leading edge, the distribution of Ed in the DME cells becomes polarized in the plane of the tissue (Fig. 1 E′). In both $ed^{M/Z}$ and Ed-AS embryos, the planar polarized distribution of Ed in the DME cells is eliminated; Ed is absent from all DME cell interfaces in $ed^{M/Z}$ embryos and present at all DME cell interfaces in Ed-AS embryos. We therefore propose that the planar polarized distribution of Ed, rather than simply its presence or absence, is necessary for the normal regulation of the actin cytoskeleton and cell shape in DME cells.

Planar polarity of the DME cells is not disrupted in $ed^{M/Z}$ and Ed-AS embryos

To determine whether DME cell planar polarity is generally disrupted in $ed^{M/Z}$ and Ed-AS embryos, we investigated the distribution of other polarized proteins. For example, septate junctions are present at contacts between epidermal cells but are lost from the leading edge during dorsal closure (Fig. 2 J; Magie et al., 1999; Kaltschmidt et al., 2002). In both $ed^{M/Z}$ and Ed-AS embryos, the localization of septate junction markers Coracle and Discs Large is indistinguishable from wild type (Fig. 2, J–L and not depicted). In addition, the nonclassical cadherin Flamingo (Fmi), a component of the planar polarity core complex, displays a similar planar polarized distribution (Fig. 2 M; Kaltschmidt et al., 2002), which is also unaffected in both $ed^{M/Z}$ and Ed-AS embryos (Fig. 2, N and O). Together these data indicate that the defects in actomyosin cable formation in $ed^{M/Z}$ and Ed-AS embryos do not reflect an overall disruption of DME cell planar polarity and suggest that asymmetric distribution of Ed in the DME cells is specifically required for the planar polarization of the actin cytoskeleton.

Asymmetric localization of Ed is required for the planar polarized distribution of actin regulators in DME cells

Actomyosin cable formation during dorsal closure requires the accumulation of known regulators of actin filament assembly and contractility at the leading edge (Harden et al., 1999; Magie et al., 1999; Wood et al., 2002; Homem and Peifer, 2008). To investigate how altering Ed distribution might interfere with cable formation, we examined the distribution of such factors in $ed^{M/Z}$ and Ed-AS embryos. We reasoned that if Ed functions upstream of these regulators, then their localization within the DME cells will be disrupted. Alternatively, Ed might function downstream of or in parallel to these factors.

We looked at the distribution of RhoGEF2, one of the guanine nucleotide exchange factors known to activate the Rho small GTPase Rho1 in *Drosophila* (Grosshans et al., 2005), because actomyosin cable assembly requires signaling from Rho1 (Harden et al., 1999; Magie et al., 1999; Wood et al., 2002). Wild-type embryos exhibit an enrichment of RhoGEF2 at the leading edge during dorsal closure at the stages when the actomyosin cable is present (Fig. 3 A), which is consistent with local activation of Rho1 at the leading edge. This RhoGEF2 accumulation is abolished in both Ed-AS and $ed^{M/Z}$ embryos (Fig. 3, A′ and A′′). Similarly, Diaphanous (Dia), a formin that functions as a Rho1 effector and nucleates and elongates unbranched actin filaments (Pruyne et al., 2002; Sagot et al., 2002; Grosshans et al., 2005; Pollard, 2007) accumulates at leading edge actin-nucleating centers (ANCs) during wild-type dorsal closure (Fig. 3, B and B′, arrows; Kaltschmidt et al., 2002; Homem and Peifer, 2008) but not in $ed^{M/Z}$ embryos or adjacent to Ed-ΔC–expressing amnioserosa cells in embryos expressing Ed-ΔC in *paired* stripes (Fig. 3, B, B′ [arrowheads], and C). Enrichment of the actin regulator Enabled/VASP (Ena) at the ANCs (Fig. 3 D; Gates et al., 2007) is also abolished in Ed-AS and $ed^{M/Z}$ embryos (Fig. 3, D′ and D′′). Ena is dispensable for actomyosin cable assembly but influences actin filament stability in the leading edge filopodia (Gates et al., 2007), which is consistent with the lack of filopodia in Ed-AS and $ed^{M/Z}$ embryos (Fig. 2, B and C). Together these observations indicate that the polarized distribution of Ed within the DME cells is necessary for proper accumulation of actin regulators at their

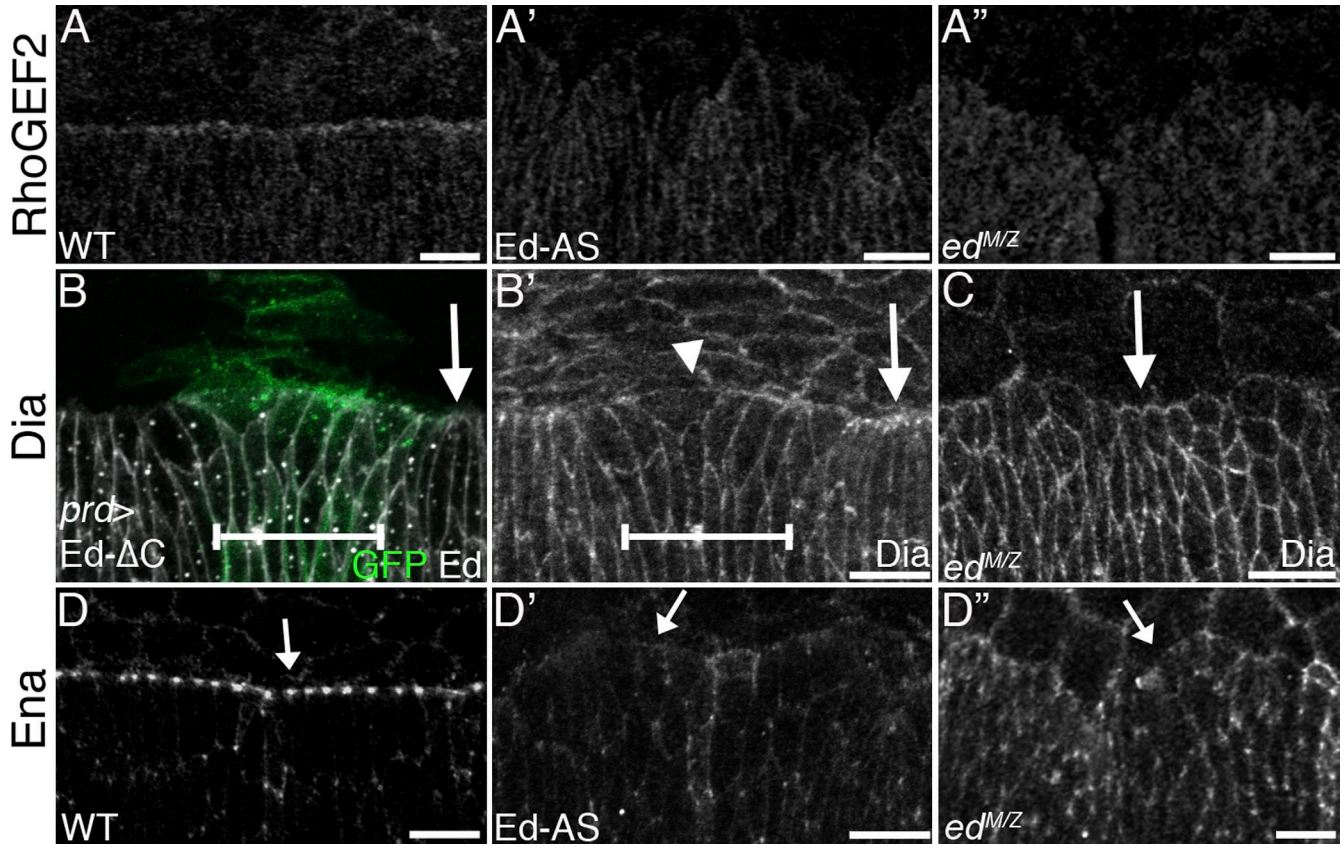

Figure 3. **Polarized distribution of Ed is essential for the planar polarization of actin regulators in the DME cells.** (A–A″) Distribution of RhoGEF2 in zippering phase wild-type (WT; A), Ed-AS (A′), and $ed^{M/Z}$ (A″) embryos. (B and B′) Embryo expressing Ed-ΔC in *paired* expression stripe pattern, giving rise to a circumferential stripe of Ed-AS cells (bars) flanked by wild-type cells (arrows), stained for Ed (B, white), GFP (B, green), and Dia (B′). Dia is enriched at the ANCs in wild-type cells but not enriched at the leading edge of Ed-AS DME cells (arrowhead). (C) Zippering phase $ed^{M/Z}$ embryo shows no enrichment of Dia at the ANCs (arrow). (D–D″) Distribution of Ena in zippering phase wild-type (D), Ed-AS (D′), and $ed^{M/Z}$ (D″) embryos. Ena is enriched at the ANC of wild-type embryo DME cells (D, arrow) but not in Ed-AS or $ed^{M/Z}$ (D′ and D″, arrows) embryos. Bars, 10 µm.

leading edge, which in turn promotes actomyosin cable and filopodia assembly.

The polarized distribution of Ed in DME cells affects the localization of Baz

As another candidate Ed effector, we looked at the distribution of the polarity protein Baz, which can interact with Ed via the Ed PDZ-binding motif (Wei et al., 2005). In wild-type embryos, Baz is detectable at all faces of the DME cells during initiation phase (Fig. 4 A′, arrow) but is gradually lost from the leading edge as the embryo proceeds to sweeping phase (Fig. 4 B′, arrow), resembling spatially and temporally the loss of Ed from this interface (Fig. 4, A and B).

During their removal from the leading edge, Ed and Baz exhibit three interesting staining patterns (Fig. 4 G). In most DME cells (46%), Ed and Baz appear to extend uniformly along the leading edge (n = 276; Fig. 4 G, uniform). In others (37%), Baz is enriched in a large focus at the middle of the leading edge (n = 276; Fig. 4 G, aggregate); Ed also appears somewhat enriched in these aggregates. In some cells (17%), this focus of Baz appears elongated along the DV axis of the DME cell (n = 276; Fig. 4 G, internalization); Ed appears mildly enriched in these foci. Although the relevance of these patterns is not clear, based on their shape and position, we speculate that they may reflect the internalization of Baz/Ed aggregates into the cytoplasm of the DME cell as Baz and Ed disappear from the leading edge. Later, during sweeping, Baz becomes enriched approximately halfway along the AP interfaces between DME cells (Fig. 4 B′, inset).

We then further examined the onset of Ed and Baz planar polarity and its relationship to actin cable formation by analyzing wild-type embryos coimmunostained for Ed, Baz, and MHC. From initiation to sweeping stage, we found a strong temporal correlation between Ed and Baz localization. In most DME cells (88%), Ed and Baz are either both present or both absent at the leading edge (n = 1,239; Fig. 4 F), making it difficult to conclude whether loss of Ed precedes the loss of Baz. We then asked whether the localization of Baz is influenced by the distribution of Ed. In both $ed^{M/Z}$ and Ed-AS embryos, Baz displays a wild-type cortical distribution during initiation (not depicted) but fails to be redistributed during the sweeping phase, remaining at the leading edge of DME cells (Fig. 4, D′ and E′). These results suggest that the asymmetric distribution of Ed is essential for the planar polarized localization of Baz in DME cells during dorsal closure. Consistent with this interpretation, during the termination phase, when the two lateral sheets of epidermis join at the dorsal midline, Ed accumulates at the new contacts created between the epidermal

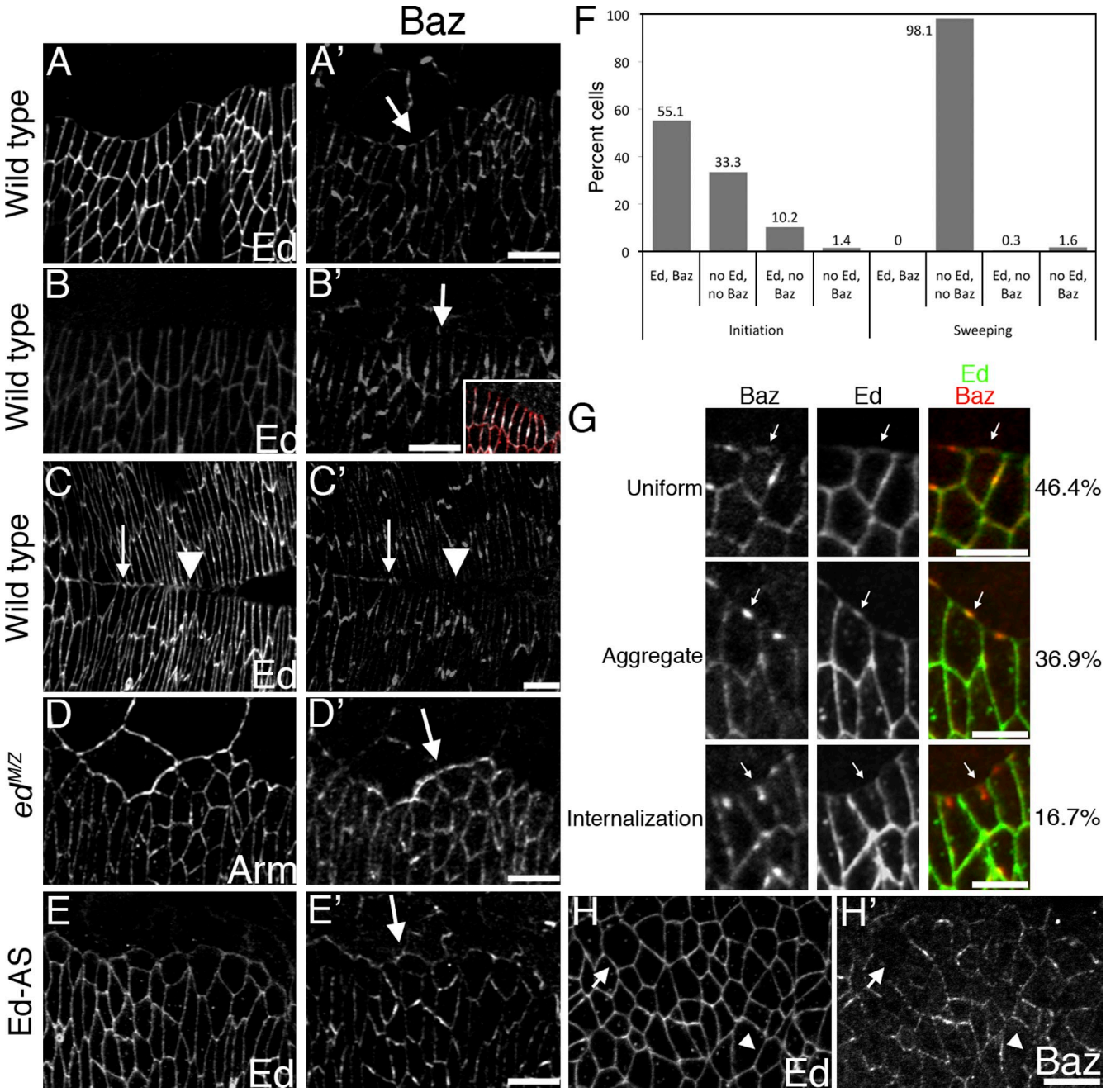

Figure 4. **Polarized Ed distribution controls the distribution of Baz at the leading edge.** (A–C′) Wild-type embryos at initiation (A and A′), sweeping (B and B′), and zippering (C and C′) phase stained for Ed (A–C) and Baz (A′–C′). During wild-type dorsal closure, Baz is gradually lost from the leading edge of DME cells (A′ and B′, arrows) and becomes enriched along the AP membranes of DME cells (B′, inset; red, Ed; white, Baz). At the end of dorsal closure when cells meet at the dorsal midline, Baz reappears at the cell contacts (C and C′, arrows) later than Ed (C and C′, arrowheads). (D and D′) ed^{MZ} embryo maintains Arm (D) and Baz (D′) at the leading edge of DME cells during dorsal closure (D′, arrow). (E and E′) Ed-AS embryo stained for Ed (E) and Baz (E′) maintains Baz at the leading edge during dorsal closure (E′, arrow). (F) Percentage of DME cells showing the presence of Ed and/or Baz at their leading edge in initiation (n = 412 cells) or sweeping (n = 938 cells) phase. (G) Early sweeping phase embryos stained for Baz (left), Ed (middle), and merge (right; green, Ed; red, Baz) showing the observed frequencies of each distribution pattern (uniform, aggregate, and internalizing) at the leading edge. (H and H′) Wild-type germ band extension embryo stained for Ed (H) and Baz (H′). Ed is uniform (H, arrow and arrowhead), whereas Baz is polarized (H′, arrow and arrowhead). Bars: (A′–E′ and H′) 10 µm; (G) 5 µm.

cells (Fig. 4 C, arrowhead) before the appearance of Baz, which is detectable in mature contacts more distal to the zippering front (Fig. 4 C′, arrow).

When we analyzed the distribution of MHC in these embryos, the temporal relationship was more clear. MHC is never up-regulated at the DME cell leading edge while Ed is still present there (n = 979 DME cells from late initiation to early zippering embryos), indicating that the loss of Ed from the leading edge and the consequent planar polarized distribution of Ed and Baz precede actomyosin cable assembly. Together with our observation that altering the distribution of Ed disrupts MHC accumulation at the leading edge, these data support the hypothesis that

the polarized localization of Ed and/or Baz leads to actomyosin cable formation.

The loss of Baz and enrichment of MHC at the epidermal leading edge during dorsal closure is reminiscent of their polarized distribution during the epithelial cell intercalation events that drive germ band extension, where MHC accumulates at the shrinking AP interfaces and Baz becomes enriched at DV interfaces (Bertet et al., 2004; Zallen and Wieschaus, 2004). The epidermal leading edge during dorsal closure thus resembles the AP interfaces during germ band extension, both in its enrichment of MHC and its contraction. However, in contrast to dorsal closure, we did not observe a corresponding planar polarized localization of Ed in the epidermis in embryos during germ band extension (Fig. 4, H and H′). Therefore, although Ed can regulate the planar polarized localization of Baz and MHC during dorsal closure, the uniform distribution of Ed during germ band extension suggests that different factors contribute to their polarization during this process.

The Ed intracellular domain but not the PDZ-binding motif is required for actomyosin cable formation

Our data support a model in which the planar polarized distribution of Ed influences the organization of the actin cytoskeleton, directing actomyosin cable formation to the epidermal leading edge during dorsal closure. A simple prediction of this model is that in the cells with the planar polarized distribution of Ed, the Ed intracellular domain will be required for localized actomyosin cable assembly. To test this idea, we induced clones of *ed* mutant cells in the ovarian follicular epithelium to create ectopic interfaces between wild-type Ed-expressing cells and *ed* mutant cells. Such interfaces are analogous to the epidermis/amnioserosa interface in terms of differential Ed expression, smooth morphology, and enrichment for actomyosin cable markers (Laplante and Nilson, 2006). These interfaces also lack detectable Ed, and therefore, the wild-type cells abutting the clone border exhibit a planar polarized distribution of Ed (Laplante and Nilson, 2006). Thus, in many aspects, these cells resemble DME cells during dorsal closure. However, in the follicle cell clone system, the Ed-expressing and nonexpressing cells are of the same cell type, confirming that the interface phenotypes result from differences in Ed expression rather than differences in cell type.

To manipulate Ed expression in this system, we used the mosaic analysis with a repressible cell marker (MARCM) system (Lee and Luo, 2001) to generate mitotic clones of homozygous *ed* mutant follicle cells that also express GAL4, which in turn drives expression of a UAS-GFP marker and a UAS-Ed transgene exclusively in the *ed* mutant cells. In terms of Ed expression, expression of transgenic Ed in *ed* mutant cells is analogous to ectopic expression of Ed in the amnioserosa. As predicted, expression of Ed-Full in *ed* mutant clones rescues the *ed* mutant phenotype; the clone border is not smooth and does not exhibit enriched pMLC (29/29 interfaces in 21 egg chambers; Fig. 5, A and A′, arrows). This rescue occurs even though Ed-Full is expressed at considerably higher levels than endogenous Ed in the wild-type cells (Fig. 5 A), indicating that a difference in Ed levels between neighboring cells is not sufficient to trigger cable formation, and is consistent with our previous observation that a smooth boundary is not observed between cells with one and two copies of wild-type *ed* (Laplante and Nilson, 2006). The same phenotype is observed with Ed-ΔP (14/14 interfaces in 15 egg chambers; Fig. 5, B and B′, arrows). Consistent with our analysis of dorsal closure, expression of Ed-ΔC in *ed* mutant cells maintains endogenous Ed in the nonmutant cells at this interface and abolishes the smooth interface phenotype (21/21 interfaces in 21 egg chambers; Fig. 5, C–C′′, arrows), further supporting the hypothesis that the planar polarized distribution of Ed leads to localized actomyosin cable formation.

When analyzing these mosaic epithelia, we noted that a subset of the *ed* mutant follicle cells occasionally fail to express the transgene. The cause of this lack of expression is unknown, but we can identify these cells unambiguously through their lack of Ed staining. Such events are useful because they generate interfaces between cells lacking Ed and cells expressing transgenic Ed, allowing us to ask whether the polarized distribution of truncated forms of Ed can lead to actomyosin cable assembly at the clone border. As predicted, at interfaces between *ed* mutant cells lacking Ed and *ed* mutant cells expressing transgenic Ed-Full, a smooth border and an actomyosin cable are detected (41/41 interfaces in 21 egg chambers; Fig. 5, A and A′, arrowheads). The same phenotype was observed at interfaces between cells lacking Ed and those expressing Ed-ΔP (42/42 interfaces in 15 egg chambers; Fig. 5, B and B′, arrowheads), indicating that, although previous work has invoked a role for the PDZ-binding motif of Ed in cable assembly through its ability to interact with Baz and the actin-interacting protein Canoe (Wei et al., 2005), Ed-ΔP behaves like Ed-Full in this assay. However, interfaces between *ed* mutant cells expressing Ed-ΔC and those that fail to express the transgene, and therefore lack Ed, remain jagged, and no actomyosin cable is detected (17/17 interfaces in 21 egg chambers; Fig. 5, D–D′′, arrows), indicating that the Ed intracellular domain is required in the Ed-expressing cell for actomyosin cable assembly at the interface. These data indicate that the Ed cytoplasmic domain but not the PDZ-binding motif is required for regulation of the actin cytoskeleton by the polarized distribution of Ed (Fig. 6).

Discussion

Loss of Ed from the amnioserosa triggers actomyosin cable assembly at the epidermal leading edge

Our data demonstrate that an actomyosin cable forms at the epidermal leading edge because the disappearance of Ed from the amnioserosa generates an interface between cells with Ed (the epidermis) and those without Ed (the amnioserosa). Ectopic expression of transgenic Ed in the amnioserosa abolishes cable formation at the leading edge of the epidermis, indicating that loss of Ed is required to induce cable assembly. Moreover, creating ectopic interfaces between cells with and without Ed, by generating *ed* mutant clones in the follicular epithelium, also leads to cable formation (Laplante and Nilson, 2006), indicating that differential expression of Ed, as opposed

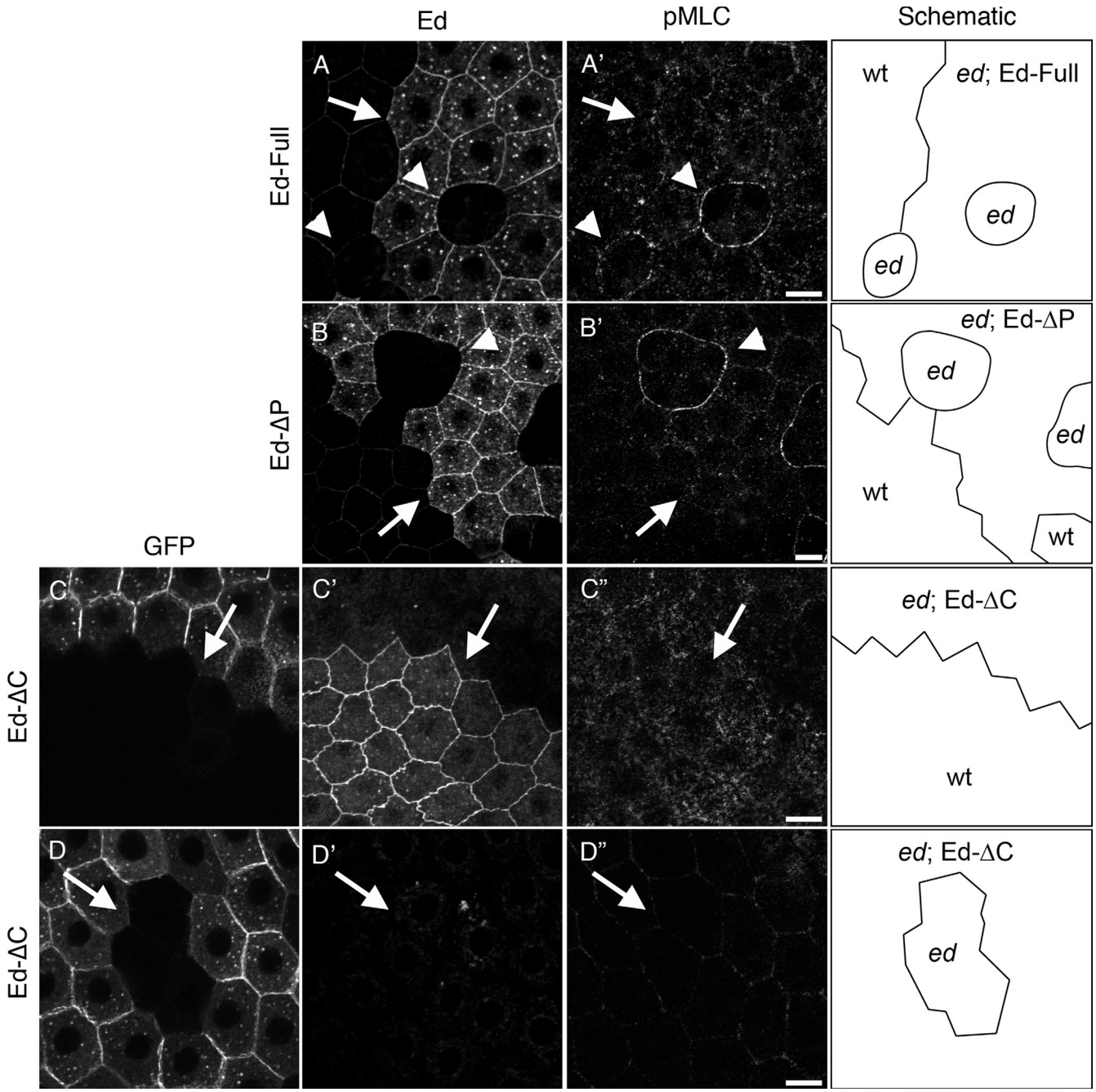

Figure 5. **The PDZ-binding motif of Ed is dispensable for actomyosin cable assembly.** (A–D″) Mosaic follicular epithelia with MARCM clones were stained for Ed (A, B, C′, and D′) and pMLC (A′, B′, C″, and D″). The clones express Ed-Full (A and A′), Ed-ΔP (B and B′), or Ed-ΔC (C–D″). Diagrams (right) illustrate the different cell genotypes within the mosaic epithelia. Arrows indicate interfaces between *ed* mutant cells expressing an Ed transgene and wild-type (wt) cells with endogenous Ed. Arrowheads indicate interfaces between *ed* mutant cells expressing an Ed transgene and *ed* mutant cells that do not express Ed (no-Ed). (A and A′) Ed/no-Ed and Ed-Full/no-Ed interfaces are smooth and exhibit an actomyosin cable; Ed-Full/Ed interfaces do not show this phenotype. (B and B′) Ed-ΔP is indistinguishable from Ed-Full in this assay. (C–C″) Expression of Ed-ΔC, which bears a GFP tag, in *ed* mutant clones stabilizes endogenous Ed at the clone border (C′); the Ed/Ed-ΔC interface is not smooth and no cable forms. (D–D″) Unlike Ed-Full/no-Ed interfaces, Ed-ΔC/no-Ed interfaces are not smooth and do not exhibit a cable. There is no signal in D′ because the anti-Ed antiserum does not recognize Ed-ΔC. Bars, 10 µm.

to other cell type–specific differences, is sufficient for this effect. Although a previous study suggested that ectopic expression of Ed in the amnioserosa does not affect actomyosin cable assembly (Lin et al., 2007), this discrepancy may reflect the fact that that work used a full-length Ed transgene, which we show is not expressed efficiently in pAS cells. Differential expression of Ed between DME cells and the adjacent amnioserosa cells may therefore have been maintained in those experiments, thus explaining the observed failure to block actomyosin cable formation. Our analysis of Ed function in dorsal closure indicates that in multiple developmental contexts, the juxtaposition of Ed-expressing and -nonexpressing cells leads to actomyosin cable formation at their interface (Laplante and Nilson, 2006).

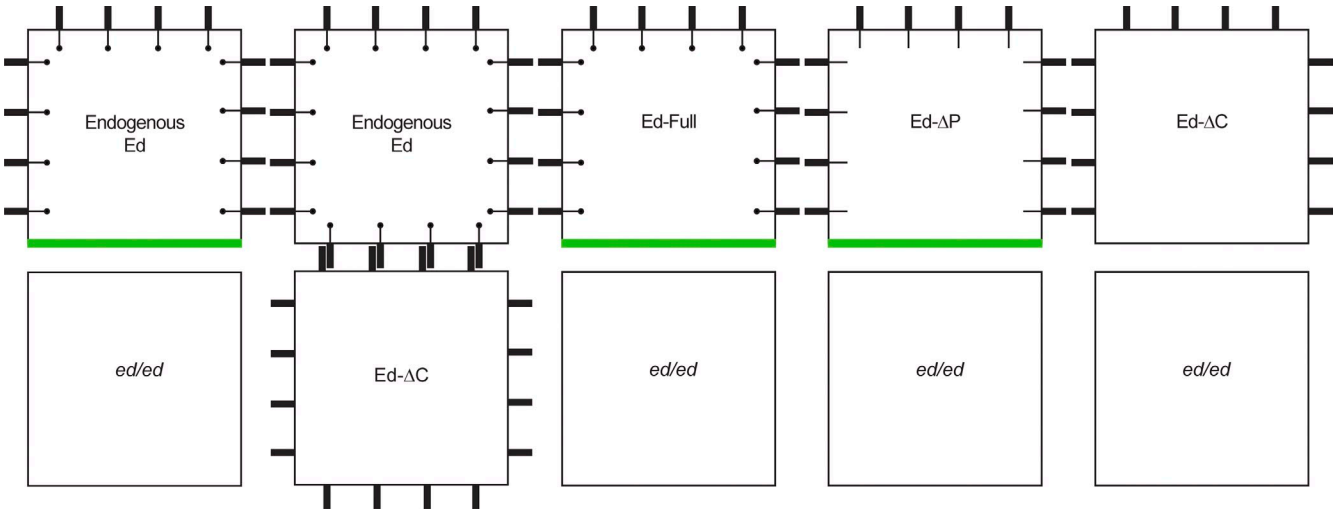

Figure 6. **Localized actomyosin cable formation requires the polarized distribution of Ed and the Ed intracellular domain.** (left to right) Interfaces between wild-type (endogenous Ed) and *ed* mutant (*ed/ed*) cells display an actomyosin cable (green). Ectopic expression of Ed-ΔC in *ed/ed* cells retains endogenous Ed at the interface and abolishes cable formation. When *ed/ed* follicle cells expressing transgenic Ed abut cells lacking Ed, both Ed-Full and Ed-ΔP can mediate cable formation but Ed-ΔC cannot, indicating that the Ed intracellular domain, but not the PDZ-binding motif, is required for induction of actomyosin cable assembly by the polarized distribution of Ed.

The ability of the absence of Ed from the amnioserosa to influence the actin cytoskeleton of the neighboring DME cells is a consequence of the homophilic binding properties of Ed. Loss of Ed from the amnioserosa eliminates Ed-mediated homophilic interactions with the adjacent DME cells, leading to the disappearance of Ed from their leading edge. Absence of Ed from the leading edge is in turn required for cable formation because ectopic expression of Ed-ΔC in the amnioserosa is sufficient to retain Ed at the leading edge and abolish cable formation. The absence of Ed from the amnioserosa thus provides the positional cue that molecularly distinguishes the epidermal cells that lie at the leading edge of the tissue: the DME cells are the only epidermal cells that abut Ed-nonexpressing cells and consequently have a planar polarized distribution of Ed.

Based on these observations, we propose that the function of Ed in this context is to act as a sensor, detecting through its homophilic binding capability whether its neighbors also express Ed, and thus providing information to the cell about its position within the tissue. Homophilic binding is typically interpreted as mediating cell adhesion, and indeed, Ed can mediate aggregation in an S2 cell assay (Islam et al., 2003; Spencer and Cagan, 2003). However, loss of Ed in vivo does not result in any physically apparent defects in adhesion (Wei et al., 2005; Laplante and Nilson, 2006). The smooth border of *ed* mutant clones has been proposed to reflect differential adhesion of wild-type and mutant cells (Wei et al., 2005), but we show that expression of different levels of Ed between neighboring cells does not generate a smooth interface or result in cell sorting. Therefore, we speculate that the homophilic binding ability of the Ed extracellular domain may reflect a recognition function rather than a role in cell adhesion. Alternatively, Ed might serve both functions simultaneously; for example, subtle alterations in adhesion could underlie the cytoskeletal and morphological changes that occur at Ed/no-Ed interfaces. In addition, Ed may serve different functions in different developmental contexts, such as those with no apparent differential expression of Ed (Bai et al., 2001; Escudero et al., 2003; Hortsch, 2003; Rawlins et al., 2003a,b; Spencer and Cagan, 2003; Swan et al., 2006; Laplante et al., 2010).

The polarized distribution of Ed establishes the planar polarity of the actin cytoskeleton

The assembly of the actomyosin cable at the leading edge upon the loss of Ed could imply that Ed functions locally to negatively regulate cable assembly. However, such a scenario would predict that embryos that lack Ed entirely would exhibit actomyosin cable assembly at all epidermal interfaces, and we do not detect this effect in $ed^{M/Z}$ embryos. Moreover, *ed* mutant cells in mosaic follicular epithelia exhibit cable formation only where they abut neighboring Ed-expressing cells and not at interfaces with adjacent *ed* mutant cells (Laplante and Nilson, 2006). Also inconsistent with such a hypothesis is our observation that both $ed^{M/Z}$ embryos, which lack Ed altogether, and Ed-AS embryos, which retain Ed at the DME cell leading edge, fail to accumulate actin regulators and to assemble an actomyosin cable. A common feature of these two situations is the loss of the planar polarized localization of Ed in the DME cells; Ed is uniformly present in Ed-AS embryos and uniformly absent in $ed^{M/Z}$ embryos. Therefore, we favor instead the hypothesis that the planar polarized distribution of Ed within the DME cells, which results from a loss of Ed from the amnioserosa, directs cable assembly to the leading edge. This process appears to be independent of the JNK pathway because expression of a JNK pathway reporter is unchanged in $ed^{M/Z}$ embryos (Lin et al., 2007) and Ed expression is unaffected in embryos with JNK pathway defects (unpublished data). Localized actomyosin cable assembly requires the Ed intracellular domain because follicle cells with a polarized distribution of Ed-ΔC do not exhibit a cable or a smooth interface with neighboring *ed* mutant

cells. Interestingly, the Ed PDZ-binding motif is not required for Ed function in this process, although several known PDZ domain–containing proteins, such as Baz and Cno, can interact with Ed through this motif. However, this region may be important for Ed function in other processes (Swan et al., 2006; Lin et al., 2007).

The distribution of Ed is important for establishing the planar polarity of the actin cytoskeleton but is not required for the overall planar polarity of the DME cells. Distinct aspects of DME cell planar polarity are thus genetically separable, suggesting that Ed functions downstream of, or in parallel to, other DV positional information that defines DME cell polarity. The nature of this additional information, however, is unknown. For example, although the Wingless signaling pathway is required for establishment of multiple aspects of DME cell planar polarity, it functions in a permissive rather than an instructive manner and does not provide spatial information (Kaltschmidt et al., 2002). Therefore, Ed is the first example of a spatial cue that establishes, at least in part, DME cell planar polarity.

It has recently been shown that Ed is required for proper ommatidial rotation in the retinal epithelium of the eye imaginal disc, which establishes planar polarity in this tissue (Fetting et al., 2009; Ho et al., 2010). One study proposes that Ed functions in this process through regulation of Fmi internalization in interommatidial cells and that the consequent up-regulation of Fmi in these cells in the absence of Ed can account for the misrotation of photoreceptor clusters in *ed* mutant discs (Ho, 2010). In the embryo, however, our data show that Fmi exhibits a wild-type planar polarized distribution in both $ed^{M/Z}$ and Ed-LE DME cells, suggesting that Ed does not regulate Fmi distribution in this context.

Baz functions downstream of Ed and upstream of polarized myosin enrichment

Ed may regulate cable formation by influencing the localization of Baz. We show that wild-type embryos exhibit a planar polarized distribution of Baz in the DME cells during dorsal closure. Like Ed, Baz disappears from the leading edge and therefore exhibits a planar polarized distribution that is complementary to that of the actomyosin cable. Manipulating the distribution of Ed, as in $ed^{M/Z}$ and Ed-AS embryos, generates a uniform distribution of Baz within the DME cells, suggesting that Ed localization influences that of Baz and therefore acts upstream. This relationship is likely to be indirect because it is the polarized distribution of Ed, rather than simply its presence or absence, that is required for normal Baz localization.

A wild-type planar polarized distribution of Baz may in turn direct localized actomyosin cable formation. The complementary polarized localization of Baz and the actomyosin cable during dorsal closure is reminiscent of their planar polarized distributions during germ band extension, when Baz and MHC are enriched at reciprocal faces of ectodermal cells (Bertet et al., 2004; Zallen and Wieschaus, 2004). MHC accumulates at AP interfaces where constriction occurs, whereas Baz accumulates at DV-expanding interfaces. A similar reciprocal localization is seen in the amnioserosa cells, as they elongate during gastrulation (Pope and Harris, 2008). Our data show that during dorsal closure loss of Baz from the DME cell leading edge precedes the assembly of the actomyosin cable, which is consistent with the hypothesis that Baz acts upstream of cable assembly and suggesting that the complementary localization of Baz and MHC in various morphogenetic processes may reflect regulation of the actin cytoskeleton by the distribution of Baz. Although we cannot exclude the possibility that the polarized distribution of Ed influences Baz localization and actomyosin cable assembly independently, we propose that the polarized distribution of Ed generates a polarized distribution of Baz, which in turn regulates actin cable formation.

The actin cable restricts the movement of the leading edge

The prevailing models for the function of the actin cable in dorsal closure propose that the tension associated with the cable promotes the dorsal movement of the leading edge. Initial studies suggested that the cable drives dorsal movement by providing a purse string-like force (Young et al., 1993; Kiehart et al., 2000), and more recent live imaging and modeling studies suggest that pulsed contractions of the amnioserosa cells provide the primary force driving leading edge migration and that myosin-mediated contraction of the cable instead acts to stabilize forward progress between contractions (Kiehart et al., 2000; Solon et al., 2009; Blanchard et al., 2010; David et al., 2010). These models differ, but each predicts that the leading edge would recede ventrally in the absence of the actin cable.

Our ability to specifically block cable formation through ectopic expression of Ed in the amnioserosa provides a novel tool for addressing this question. Particularly informative are embryos where we specifically abolish cable formation in alternating regions of the leading edge by expressing UAS-Ed in circumferential stripes. In such embryos, the DME cells that lack an actomyosin cable move dorsally in advance of those with an intact cable, suggesting that the cable restricts, rather than promotes, the forward movement of the leading edge. This phenotype is also seen when Rho1 function is abolished in alternating epidermal stripes, which also locally disrupts cable formation (Jacinto et al., 2002a). Together these observations suggest that the actin cable provides tension that coordinates the dorsal migration of the leading edge, thus ensuring that DME cells reach the dorsal midline in a sequential and coordinated manner and thus align with the appropriate corresponding contralateral segment. In the final stage of dorsal closure, such an alignment mechanism would be further reinforced by filopodial interactions between opposing segments at the dorsal midline (Millard and Martin, 2008).

Conclusion

Our work identifies differential expression of Ed as the event that distinguishes the DME cells and generates the planar polarity of their actin cytoskeleton, thus defining the contractile leading edge of the epidermis. Differential expression of a homophilic adhesion molecule may represent a general mechanism for distinguishing the cells at a tissue interface or boundary and initiating the subcellular changes that execute the cellular behaviors appropriate for their position.

Materials and methods

Generation of transgenes

Transgenes were generated by PCR amplification from cDNA RE66591 (*Drosophila* Genomics Resource Center [DGRC]) and inserted in the pENTR vector (Invitrogen), sequenced (Génome Québec Innovation Center), and recombined into the destination vector pTWG (for Ed-ΔC and Ed-ΔP) or pTWH (for Ed-Full; DGRC). Forward primer for all constructs, 5′-CACCC-GTGTGTGCGAACAACAACTCAG-3′; reverse primer for Ed-Full, 5′-CTAGA-CAATAATCTCGCGTATG-3′; reverse primer for Ed-ΔP, 5′-GCGTATGA-CGCGACGGTTTCTGGC-3′; reverse primer for Ed-ΔC, 5′-GCTCTTCTTC-GATTGATTGCGCTT-3′. The Ed-ΔC protein lacks the Ed cytoplasmic domain except for the first nine amino acids. Multiple transgenic lines were generated for each construct and yielded similar results.

Drosophila strains

Germline clones were generated as described previously using *w; ed^{F72} FRT40A* (Laplante and Nilson, 2006). *w; ed^{F72} FRT40A, UAS-Ed-ΔP* and *w; ed^{F72} FRT40A, UAS-Ed-Full* were generated by meiotic recombination. For ectopic expression of Ed transgenes, flies bearing c381-GAL4 (which drives expression in the amnioserosa) or *paired*-GAL4 (which drives expression in circumferential stripes; Yoffe et al., 1995) were crossed to flies bearing the UAS-Ed-Full, UAS-Ed-ΔP, or UAS-Ed-ΔC transgenes. For MARCM clones, *y w hsFlp, UAS-GFP; Tub-Gal80, FRT40A; Tub-Gal4/TM6* (provided by D. Hipfner, Institut de Recherches Cliniques de Montreal, Montreal, Quebec, Canada) was crossed to *w; ed^{F72} FRT40A, UAS-Ed-ΔP/CyO* or *w; ed^{F72}, FRT40A, UAS-Ed-ΔP/CyO*. The resulting pupae were heat shocked for 1 h on three consecutive days, and progeny were aged for 6 d and well fed before dissection.

Immunohistochemistry

Ovaries were dissected in PBS (1 mM KH_2PO_4, 154 mM NaCl, and 3 mM Na_2HPO_4), fixed at room temperature for 20 min in 4% formaldehyde (EM grade, methanol free; Polysciences, Inc.) in PBS/1% NP40 saturated with heptane, washed three times for 10 min in PBS + 0.1% Tween 20 (PBST), incubated at room temperature for 1 h in PBS with 1% Triton X-100, then blocked for 1 h in PBST + 1% BSA. Ovaries were then incubated overnight at 4°C in PBST with primary antibody, washed three times for 20 min each at room temperature in PBST, incubated for 1 h in PBST + 1% BSA, then incubated for 90 min in the dark with PBST + 1% BSA containing the appropriate secondary antibody. Samples were washed three times for 20 min in PBST, incubated for 30 min in PBST with rhodamine-conjugated phalloidin (dried of methanol and diluted 1:800 in PBST + 1% BSA; Invitrogen) and 5 min with 0.1 µg/µl DAPI (Invitrogen). After manual removal of stage 14 egg chambers, samples were mounted using SlowFade Gold Antifade medium (Invitrogen).

Before immunostaining, embryos were collected and aged at 25°C for 8–12 h after egg deposition to enrich for dorsal closure stages. For F-actin and pMLC stainings, embryos were dechorionated in 50% bleach in PBS, rinsed in water, fixed in 8% formaldehyde in PBS with 0.5 U/ml phalloidin in heptane for 30 min, hand devitellinized, washed with PBST, blocked for 1 h in PBST + 1%BSA, stained overnight at 4°C with pMLC antibody (see following paragraph for dilution), then washed with PBST and incubated overnight at 4°C with secondary antibody diluted in PBST + 1% BSA and stained for 4 h with 0.5 U/ml Alexa Fluor 555–conjugated phalloidin (dried of methanol; Invitrogen). For all other immunostaining, embryos were dechorionated in 50% bleach in PBS then rinsed with water. For fixation, 10 ml boiling hot Triton X-100 salt solution (TSS; 70 mM NaCl and 0.03% Triton X-100) was added to the dechorionated embryos in a glass scintillation vial, and the embryos were swirled for 15 s. 10 ml ice-cold TSS was then added to the embryos followed by incubation on ice for 20 min. The solution was removed and replaced with 50% methanol in heptane, and the tube was shaken vigorously by hand for ∼30 s. Only embryos that sank to the bottom of the vial after this step were collected for staining. The heptane was then removed, and the embryos were rinsed with methanol and stored at −20°C for at least 2 d before staining.

Antibodies used in this study were anti-Arm N2 7A1 supernatant (mouse; 1:100; Developmental Studies Hybridoma Bank [DSHB]), anti-Ena 5G2 supernatant (mouse; 1:200; DSHB), anti-pMLC (Thr18 Ser19; embryo staining; rabbit; 1:250; Cell Signaling Technology), anti-pMLC (Ser19; egg chamber staining; rabbit; 1:250; Cell Signaling Technology), anti-zipper (rabbit; 1:600; provided by D. Kiehart, Duke University, Durham, NC; Kiehart and Feghali, 1986), anti-Dia (rabbit; 1:2,500; provided by S. Wasserman, University of California, San Diego, La Jolla, CA; Afshar et al., 2000), anti-Ed (rat; 1:1,000; Laplante and Nilson, 2006), anti-Ed (rabbit; 1:1,000), anti–Discs Large 4F3 supernatant (mouse; 1:100; DSHB), anti-Coracle (mouse; 1:500; provided by R. Fehon, University of Chicago, Chicago, IL; Fehon et al., 1994), anti-Baz (rat; 1:1,000; provided by A. Wodarz, University of Gottingen, Gottingen, Germany; Wodarz et al., 1999), anti-Fmi #74 supernatant (mouse; 1:50; DSHB), and anti-RhoGEF2 (rabbit; 1:2,000; provided by S. Rogers, University of North Carolina at Chapel Hill, Chapel Hill, NC; Rogers et al., 2004). The recombinant Ed protein was generated and purified as described previously (Laplante and Nilson, 2006) and used to immunize rabbits. All secondary antibodies (Invitrogen) were highly cross-adsorbed Alexa Fluor–conjugated anti-IgG, preblocked against fixed embryos, and used at a final concentration of 1:1,000 overnight at 4°C.

Microscopy and image analysis

Images were acquired on a confocal microscope (LSM 510 Meta; Carl Zeiss, Inc.) on an microscope (Axiovert 200M; Carl Zeiss, Inc.; McGill Cell Imaging and Analysis Network facility) at 25°C using the following objectives: Plan Neofluar 40× 1.3 NA differential interference contrast oil, Plan Apochromat 63× 1.4 NA differential interference contrast oil, C-Apochromat 40× 1.2 NA water, and C-Apochromat 63× 1.2 NA water. Images were analyzed using the imaging software Volocity (PerkinElmer). Adjustments to brightness and contrast were minimal and were applied to the whole image.

Online supplemental material

Fig. S1 demonstrates uniform expression of Ed-ΔC in the amnioserosa in Ed-AS embryos. Fig. S2 shows length measurements for dorsal epidermal cells in wild-type, *ed$^{IM/Z}$*, and ED-AS embryos. Online supplemental material is available at http://www.jcb.org/cgi/content/full/jcb.201009022/DC1.

We thank Richard Fehon, David Hipfner, Daniel Kiehart, Steve Rogers, Steve Wasserman, Andreas Wodarz, and Jennifer Zallen for reagents and Arsida Noçka and Dragana Rakic for helpful comments on the manuscript. Monoclonal antibodies were obtained from the Developmental Studies Hybridoma Bank, developed under the auspices of the National Institute of Child Health and Human Development, and maintained by The University of Iowa Department of Biological Sciences (Iowa City, IA).

This work was supported by the Natural Sciences and Engineering Research Council of Canada, the Canadian Institutes of Health Research, and the National Cancer Institute of Canada (Research Studentship award to C. Laplante).

Submitted: 3 September 2010
Accepted: 16 December 2010

References

Afshar, K., B. Stuart, and S.A. Wasserman. 2000. Functional analysis of the *Drosophila* diaphanous FH protein in early embryonic development. *Development.* 127:1887–1897.

Bai, J., W. Chiu, J. Wang, T. Tzeng, N. Perrimon, and J. Hsu. 2001. The cell adhesion molecule Echinoid defines a new pathway that antagonizes the *Drosophila* EGF receptor signaling pathway. *Development.* 128:591–601.

Bertet, C., L. Sulak, and T. Lecuit. 2004. Myosin-dependent junction remodelling controls planar cell intercalation and axis elongation. *Nature.* 429:667–671. doi:10.1038/nature02590

Blanchard, G.B., S. Murugesu, R.J. Adams, A. Martinez-Arias, and N. Gorfinkiel. 2010. Cytoskeletal dynamics and supracellular organisation of cell shape fluctuations during dorsal closure. *Development.* 137:2743–2752. doi:10.1242/dev.045872

Boutros, M., N. Paricio, D.I. Strutt, and M. Mlodzik. 1998. Dishevelled activates JNK and discriminates between JNK pathways in planar polarity and wingless signaling. *Cell.* 94:109–118. doi:10.1016/S0092-8674(00)81226-X

Brand, A.H., and N. Perrimon. 1993. Targeted gene expression as a means of altering cell fates and generating dominant phenotypes. *Development.* 118:401–415.

David, D.J., A. Tishkina, and T.J. Harris. 2010. The PAR complex regulates pulsed actomyosin contractions during amnioserosa apical constriction in *Drosophila*. *Development.* 137:1645–1655. doi:10.1242/dev.044107

Escudero, L.M., S.Y. Wei, W.H. Chiu, J. Modolell, and J.C. Hsu. 2003. Echinoid synergizes with the Notch signaling pathway in *Drosophila* mesothorax bristle patterning. *Development.* 130:6305–6316. doi:10.1242/dev.00869

Fehon, R.G., I.A. Dawson, and S. Artavanis-Tsakonas. 1994. A *Drosophila* homologue of membrane-skeleton protein 4.1 is associated with septate junctions and is encoded by the coracle gene. *Development.* 120:545–557.

Fetting, J.L., S.A. Spencer, and T. Wolff. 2009. The cell adhesion molecules Echinoid and Friend of Echinoid coordinate cell adhesion and cell signaling to regulate the fidelity of ommatidial rotation in the *Drosophila* eye. *Development*. 136:3323–3333. doi:10.1242/dev.038422

Franke, J.D., R.A. Montague, and D.P. Kiehart. 2005. Nonmuscle myosin II generates forces that transmit tension and drive contraction in multiple tissues during dorsal closure. *Curr. Biol.* 15:2208–2221. doi:10.1016/j.cub.2005.11.064

Gates, J., J.P. Mahaffey, S.L. Rogers, M. Emerson, E.M. Rogers, S.L. Sottile, D. Van Vactor, F.B. Gertler, and M. Peifer. 2007. Enabled plays key roles in embryonic epithelial morphogenesis in *Drosophila*. *Development.* 134:2027–2039. doi:10.1242/dev.02849

Glise, B., H. Bourbon, and S. Noselli. 1995. hemipterous encodes a novel *Drosophila* MAP kinase kinase, required for epithelial cell sheet movement. *Cell.* 83:451–461. doi:10.1016/0092-8674(95)90123-X

Grosshans, J., C. Wenzl, H.M. Herz, S. Bartoszewski, F. Schnorrer, N. Vogt, H. Schwarz, and H.A. Müller. 2005. RhoGEF2 and the formin Dia control the formation of the furrow canal by directed actin assembly during *Drosophila* cellularisation. *Development.* 132:1009–1020. doi:10.1242/dev.01669

Harden, N. 2002. Signaling pathways directing the movement and fusion of epithelial sheets: lessons from dorsal closure in *Drosophila*. *Differentiation.* 70:181–203. doi:10.1046/j.1432-0436.2002.700408.x

Harden, N., M. Ricos, Y.M. Ong, W. Chia, and L. Lim. 1999. Participation of small GTPases in dorsal closure of the *Drosophila* embryo: distinct roles for Rho subfamily proteins in epithelial morphogenesis. *J. Cell Sci.* 112:273–284.

Harris, T.J., J.K. Sawyer, and M. Peifer. 2009. How the cytoskeleton helps build the embryonic body plan: models of morphogenesis from *Drosophila*. *Curr. Top. Dev. Biol.* 89:55–85. doi:10.1016/S0070-2153(09)89003-0

Ho, Y.H., M.T. Lien, C.M. Lin, S.Y. Wei, L.H. Chang, and J.C. Hsu. 2010. Echinoid regulates Flamingo endocytosis to control ommatidial rotation in the *Drosophila* eye. *Development*. 137:745–754. doi:10.1242/dev.040238

Homem, C.C., and M. Peifer. 2008. Diaphanous regulates myosin and adherens junctions to control cell contractility and protrusive behavior during morphogenesis. *Development.* 135:1005–1018. doi:10.1242/dev.016337

Hortsch, M. 2003. *Drosophila* Echinoid is an antagonist of Egfr signalling, but is not a member of the L1-type family of cell adhesion molecules. *Development.* 130:5295. doi:10.1242/dev.00852

Islam, R., S.Y. Wei, W.H. Chiu, M. Hortsch, and J.C. Hsu. 2003. Neuroglian activates Echinoid to antagonize the *Drosophila* EGF receptor signaling pathway. *Development.* 130:2051–2059. doi:10.1242/dev.00415

Jacinto, A., W. Wood, T. Balayo, M. Turmaine, A. Martinez-Arias, and P. Martin. 2000. Dynamic actin-based epithelial adhesion and cell matching during *Drosophila* dorsal closure. *Curr. Biol.* 10:1420–1426. doi:10.1016/S0960-9822(00)00796-X

Jacinto, A., A. Martinez-Arias, and P. Martin. 2001. Mechanisms of epithelial fusion and repair. *Nat. Cell Biol.* 3:E117–E123. doi:10.1038/35074643

Jacinto, A., W. Wood, S. Woolner, C. Hiley, L. Turner, C. Wilson, A. Martinez-Arias, and P. Martin. 2002a. Dynamic analysis of actin cable function during *Drosophila* dorsal closure. *Curr. Biol.* 12:1245–1250. doi:10.1016/S0960-9822(02)00955-7

Jacinto, A., S. Woolner, and P. Martin. 2002b. Dynamic analysis of dorsal closure in *Drosophila*: from genetics to cell biology. *Dev. Cell.* 3:9–19. doi:10.1016/S1534-5807(02)00208-3

Kaltschmidt, J.A., N. Lawrence, V. Morel, T. Balayo, B.G. Fernández, A. Pelissier, A. Jacinto, and A. Martinez Arias. 2002. Planar polarity and actin dynamics in the epidermis of *Drosophila*. *Nat. Cell Biol.* 4:937–944. doi:10.1038/ncb882

Kiehart, D.P., and R. Feghali. 1986. Cytoplasmic myosin from *Drosophila melanogaster*. *J. Cell Biol.* 103:1517–1525. doi:10.1083/jcb.103.4.1517

Kiehart, D.P., C.G. Galbraith, K.A. Edwards, W.L. Rickoll, and R.A. Montague. 2000. Multiple forces contribute to cell sheet morphogenesis for dorsal closure in *Drosophila*. *J. Cell Biol.* 149:471–490. doi:10.1083/jcb.149.2.471

Laplante, C., and L.A. Nilson. 2006. Differential expression of the adhesion molecule Echinoid drives epithelial morphogenesis in *Drosophila*. *Development.* 133:3255–3264. doi:10.1242/dev.02492

Laplante, C., S.M. Paul, G.J. Beitel, and L.A. Nilson. 2010. Echinoid regulates tracheal morphology and fusion cell fate in *Drosophila. Dev. Dyn.* 239:2509–2519.

Lee, T., and L. Luo. 2001. Mosaic analysis with a repressible cell marker (MARCM) for *Drosophila* neural development. *Trends Neurosci.* 24:251–254. doi:10.1016/S0166-2236(00)01791-4

Lin, H.P., H.M. Chen, S.Y. Wei, L.Y. Chen, L.H. Chang, Y.J. Sun, S.Y. Huang, and J.C. Hsu. 2007. Cell adhesion molecule Echinoid associates with unconventional myosin VI/Jaguar motor to regulate cell morphology during dorsal closure in *Drosophila*. *Dev. Biol.* 311:423–433. doi:10.1016/j.ydbio.2007.08.043

Magie, C.R., M.R. Meyer, M.S. Gorsuch, and S.M. Parkhurst. 1999. Mutations in the Rho1 small GTPase disrupt morphogenesis and segmentation during early *Drosophila* development. *Development.* 126:5353–5364.

Millard, T.H., and P. Martin. 2008. Dynamic analysis of filopodial interactions during the zippering phase of *Drosophila* dorsal closure. *Development.* 135:621–626. doi:10.1242/dev.014001

Narasimha, M., A. Uv, A. Krejci, N.H. Brown, and S.J. Bray. 2008. Grainy head promotes expression of septate junction proteins and influences epithelial morphogenesis. *J. Cell Sci.* 121:747–752. doi:10.1242/jcs.019422

Noselli, S., and F. Agnès. 1999. Roles of the JNK signaling pathway in *Drosophila* morphogenesis. *Curr. Opin. Genet. Dev.* 9:466–472. doi:10.1016/S0959-437X(99)80071-9

Pollard, T.D. 2007. Regulation of actin filament assembly by Arp2/3 complex and formins. *Annu. Rev. Biophys. Biomol. Struct.* 36:451–477. doi:10.1146/annurev.biophys.35.040405.101936

Pope, K.L., and T.J. Harris. 2008. Control of cell flattening and junctional remodeling during squamous epithelial morphogenesis in *Drosophila*. *Development.* 135:2227–2238. doi:10.1242/dev.019802

Pruyne, D., M. Evangelista, C. Yang, E. Bi, S. Zigmond, A. Bretscher, and C. Boone. 2002. Role of formins in actin assembly: nucleation and barbed-end association. *Science.* 297:612–615. doi:10.1126/science.1072309

Rawlins, E.L., B. Lovegrove, and A.P. Jarman. 2003a. Echinoid facilitates Notch pathway signalling during *Drosophila* neurogenesis through functional interaction with Delta. *Development.* 130:6475–6484. doi:10.1242/dev.00882

Rawlins, E.L., N.M. White, and A.P. Jarman. 2003b. Echinoid limits R8 photoreceptor specification by inhibiting inappropriate EGF receptor signalling within R8 equivalence groups. *Development.* 130:3715–3724. doi:10.1242/dev.00602

Ricos, M.G., N. Harden, K.P. Sem, L. Lim, and W. Chia. 1999. Dcdc42 acts in TGF-beta signaling during *Drosophila* morphogenesis: distinct roles for the Drac1/JNK and Dcdc42/TGF-beta cascades in cytoskeletal regulation. *J. Cell Sci.* 112:1225–1235.

Riesgo-Escovar, J.R., and E. Hafen. 1997. Drosophila Jun kinase regulates expression of decapentaplegic via the ETS-domain protein Aop and the AP-1 transcription factor DJun during dorsal closure. *Genes Dev.* 11:1717–1727. doi:10.1101/gad.11.13.1717

Riesgo-Escovar, J.R., M. Jenni, A. Fritz, and E. Hafen. 1996. The *Drosophila* Jun-N-terminal kinase is required for cell morphogenesis but not for DJun-dependent cell fate specification in the eye. *Genes Dev.* 10:2759–2768. doi:10.1101/gad.10.21.2759

Ring, J.M., and A. Martinez Arias. 1993. puckered, a gene involved in position-specific cell differentiation in the dorsal epidermis of the *Drosophila* larva. *Dev. Suppl.* 1993:251–259.

Rogers, S.L., U. Wiedemann, U. Häcker, C. Turck, and R.D. Vale. 2004. *Drosophila* RhoGEF2 associates with microtubule plus ends in an EB1-dependent manner. *Curr. Biol.* 14:1827–1833. doi:10.1016/j.cub.2004.09.078

Sagot, I., A.A. Rodal, J. Moseley, B.L. Goode, and D. Pellman. 2002. An actin nucleation mechanism mediated by Bni1 and profilin. *Nat. Cell Biol.* 4:626–631.

Sluss, H.K., Z. Han, T. Barrett, D.C. Goberdhan, C. Wilson, R.J. Davis, and Y.T. Ip. 1996. A JNK signal transduction pathway that mediates morphogenesis and an immune response in *Drosophila*. *Genes Dev.* 10:2745–2758. doi:10.1101/gad.10.21.2745

Solon, J., A. Kaya-Copur, J. Colombelli, and D. Brunner. 2009. Pulsed forces timed by a ratchet-like mechanism drive directed tissue movement during dorsal closure. *Cell.* 137:1331–1342. doi:10.1016/j.cell.2009.03.050

Spencer, S.A., and R.L. Cagan. 2003. Echinoid is essential for regulation of Egfr signaling and R8 formation during *Drosophila* eye development. *Development.* 130:3725–3733. doi:10.1242/dev.00605

Stronach, B., and N. Perrimon. 2002. Activation of the JNK pathway during dorsal closure in *Drosophila* requires the mixed lineage kinase, slipper. *Genes Dev.* 16:377–387. doi:10.1101/gad.953002

Strutt, D.I., U. Weber, and M. Mlodzik. 1997. The role of RhoA in tissue polarity and Frizzled signalling. *Nature.* 387:292–295. doi:10.1038/387292a0

Swan, L.E., M. Schmidt, T. Schwarz, E. Ponimaskin, U. Prange, T. Boeckers, U. Thomas, and S.J. Sigrist. 2006. Complex interaction of *Drosophila* GRIP PDZ domains and Echinoid during muscle morphogenesis. *EMBO J.* 25:3640–3651. doi:10.1038/sj.emboj.7601216

Wei, S.Y., L.M. Escudero, F. Yu, L.H. Chang, L.Y. Chen, Y.H. Ho, C.M. Lin, C.S. Chou, W. Chia, J. Modolell, and J.C. Hsu. 2005. Echinoid is a component of adherens junctions that cooperates with DE-Cadherin to mediate cell adhesion. *Dev. Cell.* 8:493–504. doi:10.1016/j.devcel.2005.03.015

Wodarz, A., A. Ramrath, U. Kuchinke, and E. Knust. 1999. Bazooka provides an apical cue for Inscuteable localization in *Drosophila* neuroblasts. *Nature.* 402:544–547. doi:10.1038/990128

Wood, W., A. Jacinto, R. Grose, S. Woolner, J. Gale, C. Wilson, and P. Martin. 2002. Wound healing recapitulates morphogenesis in *Drosophila* embryos. *Nat. Cell Biol.* 4:907–912. doi:10.1038/ncb875

Yoffe, K.B., A.S. Manoukian, E.L. Wilder, A.H. Brand, and N. Perrimon. 1995. Evidence for engrailed-independent wingless autoregulation in *Drosophila*. *Dev. Biol.* 170:636–650. doi:10.1006/dbio.1995.1243

Young, P.E., A.M. Richman, A.S. Ketchum, and D.P. Kiehart. 1993. Morphogenesis in *Drosophila* requires nonmuscle myosin heavy chain function. *Genes Dev.* 7:29–41. doi:10.1101/gad.7.1.29

Zallen, J.A. 2007. Planar polarity and tissue morphogenesis. *Cell.* 129:1051–1063. doi:10.1016/j.cell.2007.05.050

Zallen, J.A., and E. Wieschaus. 2004. Patterned gene expression directs bipolar planar polarity in *Drosophila*. *Dev. Cell.* 6:343–355. doi:10.1016/S1534-5807(04)00060-7